Analysis of the water absorption test to assess the intrinsic permeability of earthen materials

Antonin Fabbri, Lucile Soudani, Fionn Mcgregor, Jean-Claude Morel

Analysis of the water absorption test to assess the intrinsic permeability of earthen materials

Fabbri, A., Soudani, L., McGregor, F. & Morel, J-C.

Original citation & hyperlink:
Fabbri, A, Soudani, L, McGregor, F & Morel, J-C 2019, 'Analysis of the water absorption test to assess the intrinsic permeability of earthen materials' *Construction and Building Materials*, vol. 199, pp. 154-162.
https://dx.doi.org/10.1016/j.conbuildmat.2018.12.014

DOI 10.1016/j.conbuildmat.2018.12.014
ISSN 0950-0618
ESSN 1879-0526

Publisher: Elsevier

Analysis of the water absorption test to assess the intrinsic permeability of earthen materials

Antonin Fabbri[1,*], Lucile Soudani[1], Fionn McGregor[1], Jean-Claude Morel[1,2]

[1] LGCB-LTDS, UMR 5513 CNRS, ENTPE, Université de Lyon, 69100 Vaulx-en-Velin, France

[2] Centre for the Built and Natural Environment, Faculty of Engineering, Environment & Computing, Coventry University, UK

ABSTRACT:

The use and development of earth as a building material is notably constrained by its specific thermal and mechanical behaviours in relation to water, currently not considered in construction norms and technical guides. As the compressive strength decreases with the presence of water in the pores, a better understanding of the material behavior at high water content range is critical to ensure safety. The key parameter driving the flow of liquid water within earthen walls is the intrinsic permeability. In this paper, we have developed a novel analysis of the water absorption test enabling the identification of the intrinsic permeability. We have validated the new method through the comparison to permeability measurements made with an oedometer at a variable hydraulic load for samples with different dry densities. This work gives therefore the opportunity to use simple standard absorption tests to assess the intrinsic permeability of earthen materials.

Keywords: Rising damps, intrinsic permeability, earthen construction materials, rammed earth, compressed earth block.

1. Introduction

Available in many places in the world and used as a construction material for thousand years, earthen material can help to tackle the world population construction needs, at an economic level as well as at an ecological one [1]–[4]. For example, the millions of heritage rammed earth houses in Europe more than 80 years old, are a huge library of evidences of the built environment that can help modern designer to draw an architecture able to tackle the XXIth century's challenges. However, its use and development is notably constrained by its particular thermal and mechanical behaviours, which are generally not considered in construction norms and technical guides.

As it has been proven that the moister the material is, the lower is its compressive strength [5]–[9]. If the water content (weight of water divided by the weight of dry soil) is too high, it can alter the whole building stability. Therefore, it is critical to assess how vulnerable a construction with a high water content can be. To do so, it is mandatory to characterize the capacity of earthen materials to manage liquid water, which is driven by the intrinsic permeability of the material.

Earthen materials are able to hold a large amount of liquid water, compared to the other construction materials. This is actually the case when the heritage buildings experience rising damp, where the water from the ground, or accumulated at its surface, is absorbed by the wall. The Figure 1 shows a collapse of a rammed earth house in Lyon (France) after inappropriate refurbishment. The external plaster was cement based and therefore not permeable to water. The indoor face of the wall was covered by different layers of paint, glue, insulation material and plasterboard, leading to seal the rammed earth wall (Figure 1). When the wall collapsed the water content of the earth was in the range of 11%-13%, which according to [5], gives a remaining compressive strength smaller than 0.4MPa, not enough to ensure the wall stability.

Figure 1 : Collapse of a rammed earth structure with 11%-13% water content in the walls

As often regarding earthen materials, they can be considered either as soils or as construction materials, for each case a specific framework is usually used. In the case of the framework related to soils, several authors have pointed out the practical obstacles to measure the intrinsic permeability. Even if some experimental setups have been designed to overcome these difficulties [10]–[13], they remain quite sophisticated and not widespread. In [14], the Hazen formula, provides an evaluation of the intrinsic permeability from the particle size distribution ; in [15], the multiscale network approach derives the hygroscopic permeability from the water vapor permeability ; in [16], the capillary transport coefficient is approximated from the water absorption coefficient and the free water saturation.

In the case of the framework related to construction materials, the approach was rather to develop water absorption experiments [16]–[19]. For example, British standard BS 3921 [20] deals with measuring the capillary suction of water in building materials through its Initial Rate of Suction (IRS) test. It consists in measuring the water absorption of a brick per unit of surface area by immerging it in water to a depth of 3mm during 1min. This test procedure can cause mass loss due to water erosion on unstabilized samples. In order to avoid this problem, which affect the measurement of water absorption, countermeasures like the use of filter discs must be taken. In addition, several authors pointed out the inaccuracy of this test [21][22]. Consequently, the capillary coefficient, also commonly called the A-Value, is commonly preferred. It is defined by the total amount of water absorbed (in kg) per the surface in contact with water (in square meters) and per the square root of the immersion time (in seconds). Several studies focused on the determination of this coefficient for a large number of construction materials, and its link to their composition and/or their microstructure [23]. The frequently used software WUFI even takes it as an income parameter to characterize materials, through a relation between A-value and the capillary transport coefficients well described in [16]. However, as the suitability of such tool has already been questioned for earth-based material [24], it is reasonable to search for a link between the water absorption coefficient and intrinsic characteristic of the material which are commonly used in mass transport equation, like the intrinsic permeability.

In addition, although its protocol of measurement is provided by the European standard EN 1015-18, some significant variability can be observed in literature on the several ways to estimate the A-Value. In [22], [25] and [26], measurements were made on cubic samples which were weighed at 1, 2, 3, 4, 5, 10, 20, 30, 40 and 60 min following an absorption protocol similar to the one described in the BS-3921. In [23], the test was made on cylindrical samples with a diameter of 20 cm and between 1.5 and 2 cm thick. The water absorption protocol consisted in putting a basal surface of the cylinder in contact with 1cm layer of paper which remained fully saturated by water during the whole test. Samples were weighed after 10, 20, 30 minutes and 1, 4, 6, 24, 48 and 72 hours. In [27] the A-value was measured on 3 types of rammed earth materials with different earth based mortars. The samples were cubic specimens of 5cm for mortars and rammed earth blocs dimensions were 30x20x28cm^3. The absorption test was performed during approximately two days. This large variability of testing procedure leads to some difficulties to compare the results, which does not give a great confidence on the direct use of the A-Value on numerical computation in order to predict water ingress within earthen walls.

In this context, this paper aims at developing a methodology to evaluate the water diffusion coefficient and the intrinsic permeability of earthen materials using the A value. For that purpose, intrinsic permeability and A-values of compacted earth samples of densities ranging from 1.4g/cm^3 to 2.0g/cm^3 were firstly experimentally estimated. The permeability tests were performed using the oedometer with the variable hydraulic load method. To determine the A-Value, an adaptation of the EN 1015-18 procedure was developed, in order to allow its analysis through a simple analytical solution of the water mass transport equation. This approach eventually led to the establishment of the relation between the A-value and the water diffusivity, which is also related to the intrinsic permeability. The comparison between direct permeability measurements and indirect estimation through the water absorption experiments was made in the last section.

2. Materials and methods

2.1. Raw earth description

The soil used in this study was extracted in Isère, France. The soil from the same location was used to build a rammed earth house in 2011, which insure that its properties are suitable for earthen constructions. Its particle size distribution is given in Figure 3.

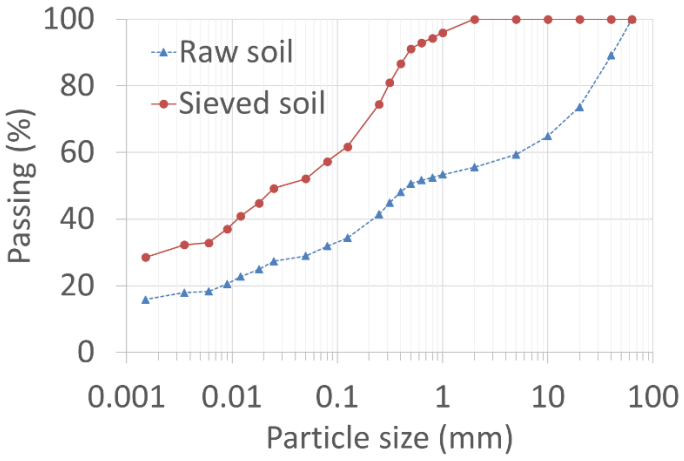

Figure 3 : Particle size distribution

It can be noticed that only 10% of grains of the raw soil have a diameter above 40 mm, which is typical of the earthen houses of this area. The points below 2µm give the clay quantity, which reaches 16% for this material.

To manufacture the samples, the raw earth was sieved at 2mm, it leads to the particle size distribution given in the Figure 3. The clay content of the sieved soil is about 30%. Its modified proctor optimum water content is 18%, for a dry density of 1.7g/cm^3. Its liquid limit is 52%, its plastic limit is 31%, and its methylene blue value is 1.7. It is thus a silty soil with no very active clays, with quite common characteristic for earthen construction.

2.2. Sample preparation and conditioning

The sieved earth was mixed with water up to a water content of 18% and wrapped in a hermetic plastic bag for at least two days before sample manufacture. The samples were manufactured in the Proctor mold, of a diameter of 10 cm with a hydraulic press.

To be as close as possible to on-site rammed earth, the target dry density of the samples was determined from several pieces of a rammed earth wallet made by a mason with the earth used in this study and prepared at a water content of 18%. It leads to the distribution of dry densities represented in Figure 4. Those seem to follow a normal law, with an average dry density of 1.67, which is quite close to the one estimated from the Proctor test. In particular, about 90% of the 23 studied samples had a density ranging from about 1.5 to 1.8. It has thus been decided to work on samples with different densities in that range. To reach the targeted dry density, the compaction force was adapted in order to fill the Proctor mold with the targeted mass soil, denoted as m_{soil}, which was calculated as follow:

$$m_{\text{soil}} = \rho_d (1 - w) V_{\text{sample}} \tag{1}$$

where V_{sample} is the sample volume (that is 471cm^3).

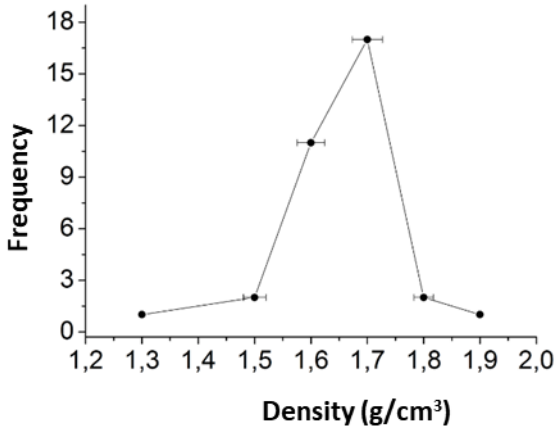

Figure 4 : Density repartition in a wallet following a Normal law

2.3. Retention curves

The retention curve expresses the link between the water content, denoted by w, that is the ratio between the mass of water within the sample and its dry mass, and the difference between gas and liquid in-pore

thermodynamic pressures, referred as the suction and denoted by s. Given the high levels of interactions between soils and water, the retention curve appears to be a key function to define the behaviour of unsaturated soils. This applies in particular to the assessment of the water absorption test since it is obvious that the suction is the driving force which induces the water penetration within the sample.

The retention curve was measured on cylindrical samples of dry density equal to 1.7 whose diameter was 15.2cm, realized with two layers of 1cm thick. The filter paper method, well experimented on soils was used (cf. for example, ASTM D5298-10 or [28]). Three dry filter papers were inserted overlaid in-between the two layers of soil during manufacture, the one in the center having a diameter about 5mm below the two others to prevent it from soil contamination. After reaching the target water content, that is 12%, 14%, 16% or 18%, the sample was sealed with plastic film and stored in a temperature regulated room at 20°C for 7 days. No control of the room relative humidity was made, but the samples were weighed before and after the equalization stage to be sure that no drying occurs during this period. After that period, the samples were destroyed with care to extract the central filter paper, the water content can then be linked to the suction through its calibration curve. Finally, the water content at saturation, denoted by w_{sat}, was estimated through the relation:

$$w_{sat} = \rho_L \left(\frac{1}{\rho_d} - \frac{1}{\rho_s} \right) \tag{2}$$

Where ρ_L is the density of water, ρ_d is the dry density and ρ_s is the grain density (that is the mass of solid per unit of solid volume), equal to 2.7 g/cm^3, which was measured with a nitrogen pycnometer (Ultrapyc 1200e). It leads to $w_{sat} = 21.7\%$.

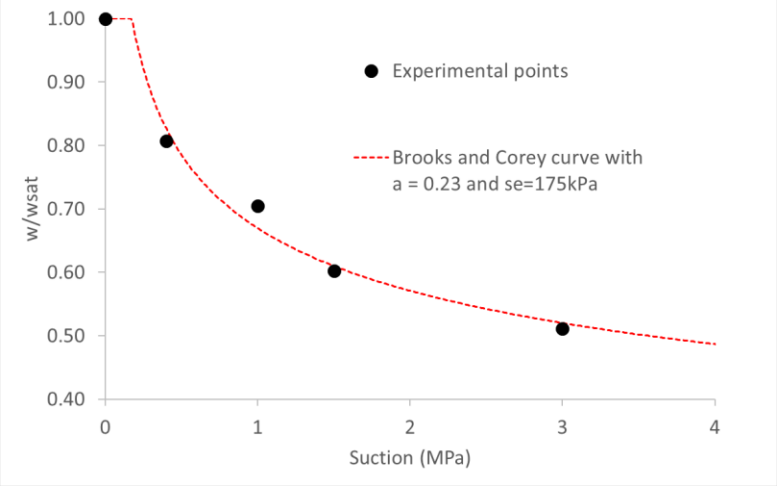

Figure 5: Retention curve at 20°C of sample compacted at the modified proctor optimal density.

Using the experimental data, reported in the Figure 5, the retention curve was obtained through the well-known Brooks and Corey equation [29]:

$$\frac{w}{w_{sat}} = \left(\frac{s}{s_e} \right)^{-a} \tag{3}$$

where w is the gravimetric water content, s is the suction, s_e is the entry air suction, a is the Brooks and Corey's coefficient and w the gravimetric water content (that is the mass of water per unit of solid mass). The Brooks and Corey equation was as it is simple to use and it gives a finite value of $\partial w / \partial s$ at $s = s_e$.

The best fit was obtained for $s_e = 175$ kPa and $a = 0.23$. It led the the curve reported in the Figure 5. These values, obtained from samples of dry density equal to 1.7 g/cm^3, are assumed to be valid for all the other samples. Thus, density variations would only modify the value of w_{sat}, but not the shape of the retention curve. This assumption is consistent with the results obtained by [30] on a soil with approximatively the same clay content as the one studied here.

2.4. Intrinsic permeability measurements

The intrinsic permeability related to liquid water, denoted by κ_0, characterises the link between the flow of water through the porous network of a saturated material and the gradient of hydraulic charge. Theoretically, the intrinsic permeability should be independent of the nature of the fluid that flows through the material. Practically, it is not the case, mainly due to the differences between fluid/solid interactions, possible slip effects for fluids of low viscosity, etc… [31]. In this paper, only the intrinsic permeability related to liquid water was considered.

For an isotropic medium we have:

$$\underline{q_L} = -\kappa_0 \frac{\rho_L g}{\eta_L} \underline{\nabla} h \tag{4}$$

were $\underline{q_L}$ is the flow of liquid, η_L the dynamic viscosity of water (=1.0 mPa.s at 20°C), ρ_L the liquid density (=1.0 g/cm^3 at 20°C), g the gravity (=9.8 N/kg), $\underline{\nabla}$ the nabla symbol, and h the hydraulic charge which is defined by:

$$h = \frac{(P_L - P_{atm})}{\rho_L g} + (z - z_0) \tag{5}$$

where P_L is the liquid pressure, P_{atm} the atmospheric pressure, z the vertical coordinate and z_0 the reference vertical coordinate at which $P_L = P_{atm}$.

In this study, the measurement of κ_0 was carried out with an oedometer following the variable hydraulic load method described in the French standard NF X 30-442. A schematic diagram of the test is represented in Figure 6. The mold, was an 11cm high cylinder with an internal diameter of 10.2cm. Samples were directly compacted within the oedometer mould using the protocol defined in the previous section.

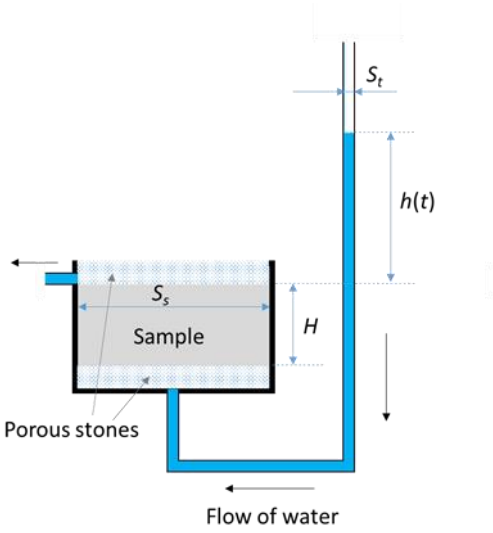

Figure 6. Schematic representation of the oedometer used for the intrinsic permeability measurements.

To avoid any loss of matter during the experimentation, geotextile discs are used at the top and bottom sides of the samples, and an axial stress of 0.01MPa is applied to the sample in order to ensure the contact between the cap of the oedometer and the sample.

During the first step, a flow of water across the sample until full saturation, was imposed. A reservoir tank was used and the sample swelling was monitored thanks to a LVDT sensor measuring the displacement of the oedometer cap. Results led to a linear swelling up to 5% for denser samples and around to 1% for lighter ones. This swelling is thus clearly not negligible, and it was taken into account for the analysis of intrinsic permeability results.

After the saturation stage, the water inflow at the bottom of the specimen was made through a capillary of cross section S_t, while the water outflow was made through a hole at the top of specimen. Under this configuration, the hydraulic charge at the top side of the sample is null while the height of the water column in the tube is directly equal to the hydraulic charge at the bottom of the sample, and the flow of liquid through the sample can thus be written as:

$$\underline{q_L} = S_t \frac{\partial h}{\partial t} \underline{e_z} \tag{6}$$

The mass conservation equation of water, combined with equations (4-6), eventually leads to the following relation between the intrinsic permeability and the height of the water column in the capillary tube:

$$\kappa_0 = \frac{\eta_L}{\rho_L g} \frac{S_t\, H}{S_s\,(t_1 - t_2)} \ln\left(\frac{h(t_2)}{h(t_1)}\right) \tag{7}$$

where S_s is the cross section of the sample, H its height while t_1 and t_2 are the times at which the height of the water column in the tube, denoted by $h(t_1)$ and $h(t_2)$ were measured.

2.5. Protocol for the water absorption experiments

The device used for the measurement of the liquid absorption coefficient (A-Value) is described in detail in [25] and it is schematized in the Figure 7A. It consisted of a tank whose bottom is covered with a bed of

gravels and sand held by a plastic grating. This layer of aggregates was immersed in a few centimeters of water. The level of water was kept constant during the whole test. When the underside of the sample was placed on this bed, it was thus in contact with water. In order to lift the sample for weighing and repositioning, a wire basket was provided. Filter discs were added between the sample and basket, and between the basket and the sand/gravel bed. The former was used to prevent particles of earth to get into the water as the sample was becoming wet, while the later insured that no sand or gravels remain hooked on the basket while it was lifted to be weighed.

To ensure a one dimensional transport of liquid water, and thus to ease the analysis of the results of the absorption test, the lateral surfaces of the samples were sealed with paraffin and aluminum foil, as can be seen in Figure 7b. Finally, the top surface was not sealed in order to avoid any in-pore gas overpressure due to the ingress of water within the porous network.

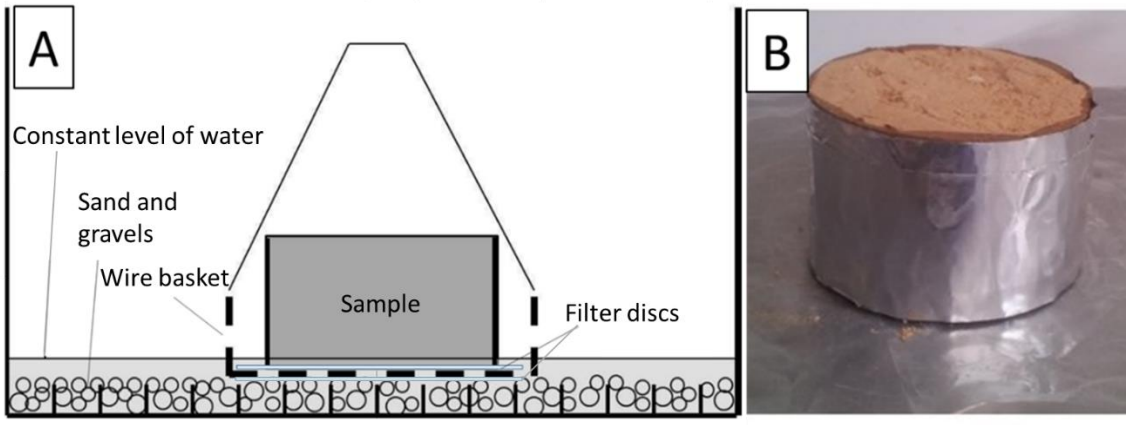

Figure 7 : A: Schematic diagram of the water absorption test (adapted from [25]). B: Sealing of the lateral faces of the samples used for the water absorption experiments

The test was made on samples initially equilibrated at 20°C and 50%RH (room temperature and relative humidity). The sample are weighed each five minutes until 60min and/or until no more mass increase was observed between two measurements. Several references ([32], [33]) highlight the fact that the weighing operation has to be done as quickly as possible. In our cases, the weighing time was between 10s and 30s. The weighing times were then subtracted from the whole time measurement.

The A-value is calculated from the slope of the linear part of the relation between the amount of absorbed water par unit of sample surface and the square root of time. It is thus expressed in $kg/m^2/s^{0.5}$.

3. Results

3.1. Intrinsic permeability measurements

The intrinsic permeability tests were made on 14 samples of initial dry density, denoted by ρ_d^0, varying between 1.44 g/cm^3 and 2.0 g/cm^3. Given the magnitude of the material swelling during the saturation process, the current dry density, denoted by ρ_d, which is the solid mass (i.e. dry mass) divided by the volume of the material after the swelling process, was calculated.

The results of intrinsic permeability tests give values between 7.3E-15 m² and 1.1E-17 m². To compare, the intrinsic permeability of permeable rocks like sandstones is commonly between 1E-12 m² and

1E-16 m² while the intrinsic permeability of non fractured argilites and concrete, which are known to be low-permeable materials, is commonly lower than 1E-19 m².

A significant variation of intrinsic permeability with density (either initial dry density, or current dry density) was observed (Figure 8A). Indeed, three orders of magnitude of variation was observed when the current density varies from 1.33 to 1.81, which is, for the record, the density variation measured in a single wall. Qualitatively, it is not surprising since intrinsic permeability is known to increase with porosity, which can be directly linked to the dry density through the relation:

$$n = 1 - \frac{\rho_d}{\rho_s} \tag{8}$$

where n is the (Euleran) current porosity (current volume of pores per unit of total current volume), ρ_d is the current dry density and ρ_s the density of the skeletton assumed to be constant.

For construction materials, the relation between intrinsic permeability and the current porosity (n) commonly follows a power law in the form [34]:

$$\kappa_0(n) = \kappa_{ref}\left(\frac{n}{n_{ref}}\right)^{\alpha} \tag{9}$$

where κ_{ref} is the reference intrinsic permeability at $n = n_{ref}$ and α is the coefficient of the power law.

Adopting $n_{ref} = 0.36$, which is the porosity at the modified proctor density (=1.7g/cm^3), the best fit was obtained with κ_{ref} =4.1E-17 m² and $\alpha = 14.8$ (cf. Figure 8B).

Such high value of α is quite unusual for construction materials: for example, Breysse and Gérard found values of α around 3 for concrete and mortar and around 6 for cement pastes [35]. According to [34], high values of α may be induced by a porous network structure composed by large pores connected to each other by narrow pressure-sensitive throats. To realise earthen samples of higher dry density, a higher compaction force is used. It may leads to the closure of these throats, which induces a drop in permeability, while the reduction in total porosity remains quite limited. Anyway, given the density heterogeneity of rammed earth walls (cf Figure 4), this strong variation of permeability with porosity would lead to quite complex water flow patterns whose shape may significanlty influence the global beaviour of the wall.

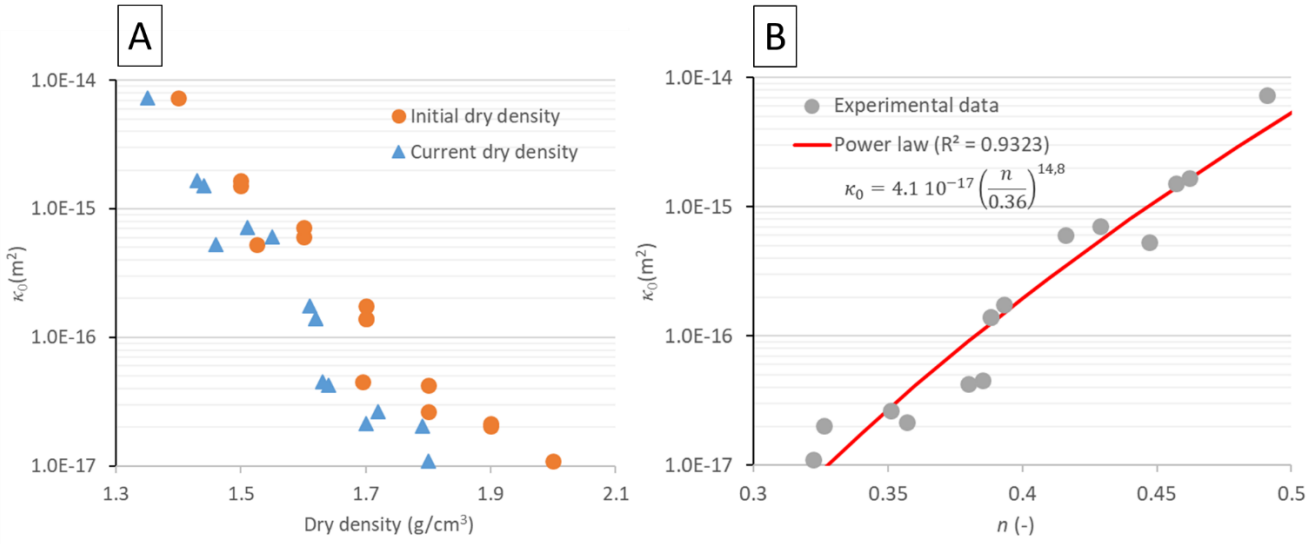

Figure 8: A: Results of the permeability tests on samples of different dry and current densities. B: Relation between the current porosity of the samples and their intrinsic permeability.

3.2. Water absorption experiments

The water absorption experiments were made on 12 samples of dry density varying between 1.4 g/cm^3 and 1.71 g/cm^3.

The amounts of water absorbed during the capillary absorption test per unit of sample cross surface in function of the square root of time are reported in the Figure 9A.

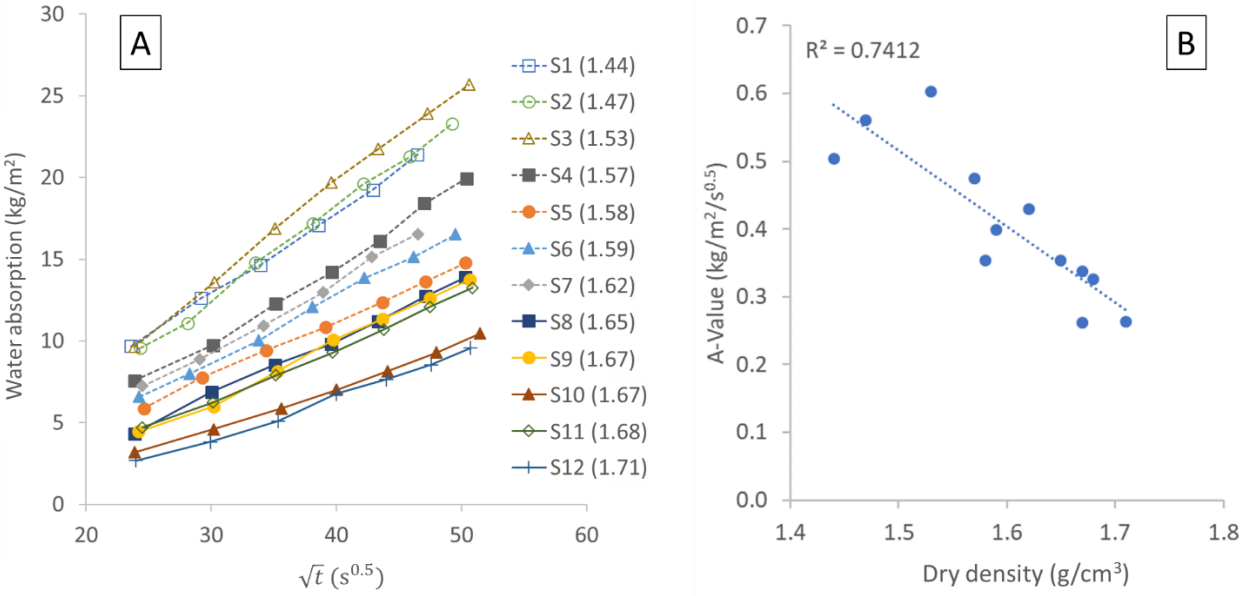

Figure 9: (A) Results of the water absorption experiments. Specific gravities of the samples are indicated in brackets; (B) Variation of the A-value with the initial dry density of the samples.

For every sample, the linearity of the relation can be noticed. The A-value, which is the slope of this line, could thus be deduced. Results are reported in Figure 9B.

Even if the results are quite scattered, a decrease of the A-value with the sample dry density is observed, which is quite intuitive. For all densities, the measured values are quite high, between 0.2 and 0.6 kg/m^2/s$^{1/2}$. Even if it remains difficult to compare directly the A-value between earthen materials since it highly depends on soil types and composition, these results are in accordance with literature data (see for example [22], [25], [27]). They are also at least one order of magnitude higher than the ones commonly obtained on cement based materials (for example 0.03 kg/m^2/s$^{1/2}$ for concrete in [26]) and in the range of clay brick values (between 0.2 kg/m^2/s$^{1/2}$ and 0.3 kg/m^2/s$^{1/2}$ in [36]). It underlines the strong capacity of the material to capture liquid water, and thus making it very sensitive to capillary issues such as rising damps.

4. Discussion

As mentioned in the introduction, the accurate use of the water absorption experiments to assess the water flows within earthen materials requires the identification of the link between the A-Value and the intrinsic permeability. For that purpose, since a relationship between the A-Value and the water diffusion can be easily made, a twostep procedure was made. The estimation of the liquid water diffusion coefficient from the absorption test was first realized before using the relationship between the water diffusion coefficient and the intrinsic permeability to draw a final relationship between the absorption tests and the intrinsic permeability

4.1. Estimation of the liquid water diffusion coefficient from the water absorption experiments

In order to analyze the link between water absorption experiments and water diffusion coefficient, we need to consider the mass conservation of the water within the sample. When a large amount of liquid water is flowing in the material, the liquid transport is prevailing upon the water vapor diffusion. In such case, assuming 1D configuration, the mass conservation of water can be written in the simplified form:

$$\frac{\partial w}{\partial t} = \frac{\partial}{\partial z}\left(D_w \frac{\partial w}{\partial z}\right) \tag{10}$$

where D_w is the water diffusion coefficient and w the water content and z the spatial coordinate.

The link between the water content and the total mass of the sample can be estimated through the equation:

$$m = S\int_0^H \rho_d w \mathrm{d}z + m_d \tag{11}$$

where m_d is the dry mass, S the cross section of the sample and H its height. The bottom of the sample, which is in contact with water, is located at $z = 0$, while the top surface of the sample, which is in contact with the atmosphere is located at $z = H$.

The combination of (10-11) leads to:

$$\frac{\partial m}{\partial t} = \frac{A}{2\sqrt{t}} = S\int_0^H \rho_d \frac{\partial}{\partial z}\left(D_w \frac{\partial w}{\partial z}\right)\mathrm{d}z = -\rho_d D_{w0}\frac{\partial w}{\partial z}(0) \tag{12}$$

where D_{w0} is the water diffusion coefficient at saturation (that is when $w = w_{sat}$) and where A is the A-value as shown in Figure 7.

If the sample height is enough, the water absorption experiment can be modelled as a 1D semi-infinite problem, with the boundary condition $w(z = 0, t) = w_{sat}$. The analytical solution of such problem, assuming that D_w is constant and equal to D_{w0}, writes in the form:

$$w(z,t) = w_{sat}\left(1 - \mathrm{erf}\left(\frac{z}{2\sqrt{D_{w0}t}}\right)\right) \tag{13}$$

where erf is the error function.

It leads to the following expression for the gradient of w at $z = 0$:

$$\frac{\partial w}{\partial z}(0) \approx -\frac{w_{sat}}{\sqrt{\pi\, D_{w0}\, t}} \tag{14}$$

The combination between (12) and (14) eventually leads to

$$D_{w0} = \pi \left(\frac{A}{2 w_{sat} \rho_d}\right)^2 \tag{15}$$

To test the validity of this approach, the variation of the sample mass during water uptake experiments, predicted using equations (10-11) with the water diffusion coefficient estimated through the equation (15) (i.e. $D_w = D_{w0}$), is compared to the experimental results. The calculation was made with the PDE module of COMSOL Multiphysic and considering the following boundary conditions:

$$w(z=0,t) = w_{sat}\ ;\ D_{w0}\frac{\partial w}{\partial z}(z=H,t) = 0 \tag{16}$$

The comparison was done for three samples S3 (ρ_d=1.53g/cm^3), S6 (ρ_d=1.59g/cm^3) and S10 (ρ_d=1.67g/cm^3). The confrontation between the numerical simulations and the experimental data, which is reported in the Figure 8, lead to a good consistency. It tends to validate the assumptions made to reach the relation (15) (i.e. constant and homogeneous water diffusion coefficient, 1D geometry, semi-infinite medium) and it gives some confidence on its applicability to estimate the liquid water diffusion coefficient of earthen materials from water absorption tests.

As it is mentioned in the introduction, another expression to estimate the link between the A-value and the water diffusivity coefficient has already been proposed in [16]. This expression, which is notably used in the software WIFI, is based on experimental observations realized by Kießl (cited by [16]) on several building materials, and it accounts for the variation of the water diffusivity coefficient with water content. To ease the reading, the water diffusion coefficient obtained with this relation will be denoted by $D_w^K(w)$ in the following of this paper, while the one obtained with the relation (15) will be denoted by D_{w0}. Using this notation, $D_w^K(w)$ writes in the form:

$$D_w^K(w) = 3.8\left(\frac{A}{\rho_d w_f}\right)^2 \cdot 1000^{\frac{w}{w_f}-1} \tag{17}$$

where w_f is the water at free saturation, which can be experimentally determined from the final mass of the sample during the absorption test: it is the water content of the sample when the plateau of the water absorption curve is reached.

The use of w_f instead of w_{sat} in the expression (17) was made to take into account that the water content at the end of the absorption test classically differs from the theoretical water content at saturation (w_{sat}). Two main reasons can explain this difference. The first one is the presence of entrapped air pockets and bubbles within the porous network. Therefore, the sample does not reach a fully saturated state at the end of the absorption test (cf. [37] for example). The second one is the swelling process of the material during the saturation stage, which can lead to a significant increase of the pore space [38]. A third one might be the gravity effect, that would induce a reduction of the water content with height [39]. But considering the size of the samples used for the capillary absorption test, this last one can reasonably be neglected.

Note that the decision to use w_{sat} instead of w_f in the expression (15) was motivated by the sake of simplicity, since a robust and accurate estimation of w_f can be quite difficult for earthen materials due to their high sensitivity to water.

A new set of simulation was made using the equation (10), but with $D_w = D_w^K(w)$, where w_f= 0.25 for the sample S3, w_f = 0.16 for the sample S6 and w_f = 0.11 for the sample S10. The following boundary conditions were considered:

$$w(z=0,t) = w_f \; ; \; D_w^K(w)\frac{\partial w}{\partial z}(z=H,t) = 0 \tag{18}$$

The results reported in Figure 10 show that the use of $D_w^K(w)$ from equation (17) instead of D_{w0} from equation (15) leads to an overestimation of the mass increase kinetics. In consequence, it seems that the equation (17) is not suitable, at least for the test conditions of this paper, to estimate accurately the water diffusion coefficient from the A-value.

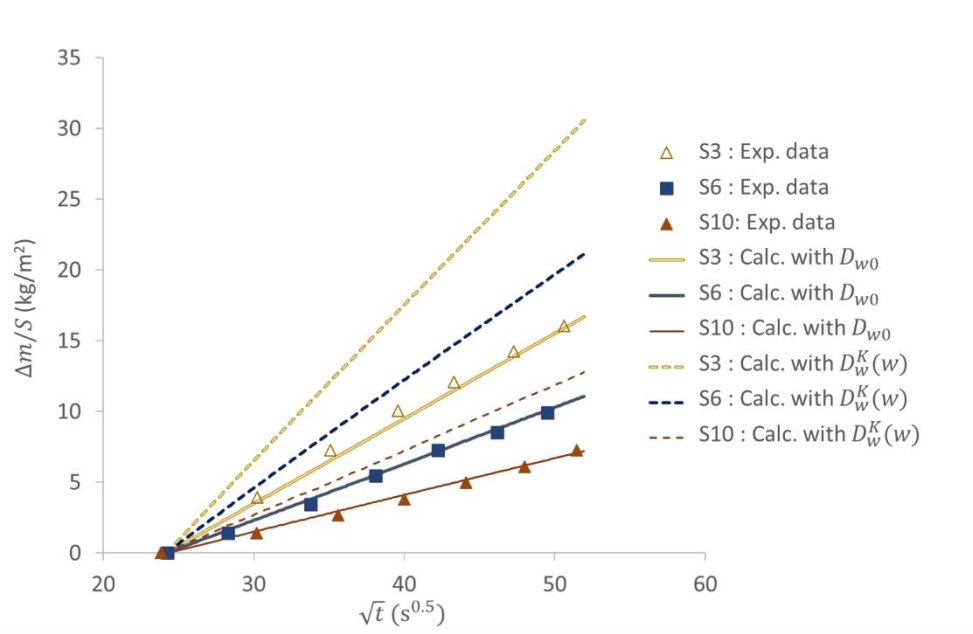

Figure 10: Simulation of the water absorption test considering either $D_w = D_{w0}$ (plain lines) or $D_w = D_w^K(w)$ (dotted lines) for the samples S3, S6 and S10 and comparison with experimental data (dots).

4.2. Link between water diffusion coefficient and intrinsic permeability

The link between the intrinsic permeability and the water diffusion coefficient writes in the form [40]:

$$\kappa_0 = -D_{w0}\frac{\rho_d}{\rho_L}\eta_L\frac{1}{\frac{\partial s}{\partial w}(w_{sat})} \tag{19}$$

where $\partial s/\partial w(w_{sat})$ is the slope of the suction curve $s(w)$ at $w = w_{sat}$ and $s = s_e$. Assuming that $s(w)$ follows the Brooks and Corey equation (3), $\partial s/\partial w(w_{sat})$ is equal to:

$$\frac{\partial s}{\partial w}(w_{sat}) = -\frac{s_e}{a\, w_{sat}} \tag{20}$$

The combination of the equations (19-20) with (15) eventually provides:

$$\kappa_0 = \pi \left(\frac{A}{2 w_s \rho_d} \right)^2 \frac{\rho_d}{\rho_L} \eta_L \frac{a\, w_{sat}}{s_e} \tag{21}$$

This expression is used to estimate the intrinsic permeability from the A-values obtained with the water absorption experiments. The results are compared to the ones obtained from the permeability tests. Since it was not possible to measure the swelling of the sample during the water absorption experiments, this comparison is made using the initial dry density of the samples and not their current dry density. Let us underline that the lateral swelling was prevented during the oedometric test. It may have not totally be the case during the absorption test, since the stiffness of the aluminium foil which sealed the sample lateral surface was lower than that of the oedometric ring. This possible difference in swelling behaviour and its impact on the permeability measurement was however neglected in this study.

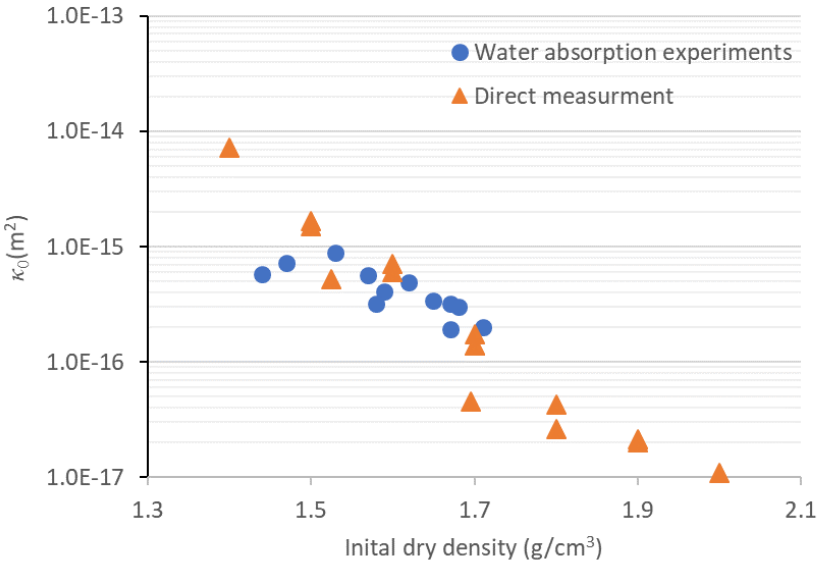

Figure 11: Comparison of intrinsic permeability values estimated from water absorption tests or permeability tests

The results are reported in Figure 11 and tend to validate the use of the equation (21) to estimate the intrinsic permeability from the water absorption experiments.

Interestingly, the permeability measurements were done after a saturation stage of the sample, and the analysis of the water absorption experiments have been made assuming a constant water diffusion coefficient. The good consistency observed between these two approaches tends to the conclusion that the water absorption experiment is driven by the water diffusion coefficient at saturation. It is logical if the water absorption phenomenon is viewed as a front penetration problem, with a binary value for the water diffusion coefficient: equal to D_{w0} downstream and equal to zero upstream. In addition, given the sharp variation of water diffusion coefficient with water content, this binary assumption seems justified. The extrapolation of this result to earthen walls would indicate that there is no need to know the variation of permeability with water content to assess rising damps phenomenon, which would considerably simplify its modelling.

To conclude, some improvement of this method would allow increasing its accuracy and its applicability. The first one would be to allow an indirect estimation of the Brooks and Corey parameters and their

variations with the dry density of the material. Another one would be to allow the measurement of the swelling process during the water absorption experiment, since that latter might not be negligible.

5. Conclusion

This paper presents the determination of intrinsic permeability of compacted earth material of several dry densities. Two experimental methods have been used. The first one consisted of the permeability tests using an oedometer test at variable hydraulic loads. It led to intrinsic permeability values ranging from 1.0E-14 m^2 to 1.0E-17 m^2 for tested initial dry densities (between 1.4g/cm^3 and 2.0g/cm^3), and higher than 1E-16 m^2 if the dry density is lower than 1.7g/cm^3, which is the modified optimum proctor density. These results confirmed the permeable nature of compacted earth materials commonly used in building construction since their density is generally lower than optimum proctor density. The experiments also underlined a strong variation of intrinsic permeability with porosity (and thus dry density), which can be accurately fitted by a power law expression of exponent 14.8. This quite high value might be induced by a particular shape of the porous network, composed by big pores connected to each other by narrow pressure sensitive pores, but more studies are needed to draw any definitive conclusions on that point.

The second set of experiments were the water absorption tests, which gives the A-value. It led to values between 0.2 kg/m^2/$s^{1/2}$ and 0.6 kg/m^2/$s^{1/2}$ which are in the range of values commonly observed for rammed earth and compacted earth blocs. This test was analysed in order to indirectly estimate the water diffusivity coefficient at saturation D_{w0} and the intrinsic permeability κ_0. For this latter, it was necessary to interpolate the retention curve of the material using the Brooks and Corey equation. The results underlined a good correlation between the two methods, which gives some confidence on the possibility to use the water absorption experiment to indirectly estimate the intrinsic permeability of earthen materials. Water absorption test is easy to perform and do not require expensive experimental devices. In consequence, the results of this paper appear to be particularly interesting for new earthen constructions and for the conservation of earthen building heritage, since this projects require a good prediction of the water behaviour within earthen walls, but most of the time the client cannot afford too complex time consuming and expensive characterisation tests.

Acknowledgments

The authors acknowledge Stephane Cointet for its technical support, as well as Barthélémy Petit and Hugo Decaudin who carry out the capillary rises and permeability experiments during their master internships.

The present work has been supported by the French Research National Agency (ANR) through the “Villes et Bâtiments Durables” program (Project Primaterre n°. ANR-12-VBDU-0001).

Bibliography

[1] J.-C. Morel, “Building with unstabilised earth in the XXI century,” in *International Symposium on Earthen Structures (ISES-2018)*, 2018.

[2] G. Habert, E. Castillo, E. Vincens, and J. Morel, “Power: A new paradigm for energy use in sustainable construction,” *Ecol. Indic.*, vol. 23, pp. 109–115, 2012.

[3] A. Arrigoni, C. Beckett, D. Ciancio, and G. Dotelli, “Life cycle analysis of environmental impact

vs. durability of stabilised rammed earth," *Constr. Build. Mater.*, vol. 142, pp. 128–136, 2017.

[4] J. C. Morel, A. Mesbah, M. Oggero, and P. Walker, "Building houses with local materials: means to drastically reduce the environmental impact of construction," *Build. Environ.*, vol. 36, no. 10, pp. 1119–1126, 2011.

[5] Q.-B. Bui, J.-C. Morel, S. Hans, and P. Walker, "Effect of moisture content on the mechanical characteristics of rammed earth," *Constr. Build. Mater.*, vol. 54, pp. 163–169, 2014.

[6] P. A. Jaquin, C. E. Augarde, D. Gallipoli, and D. G. Toll, "The strength of unstabilised rammed earth materials," *Géotechnique*, vol. 59, pp. 487–490, 2009.

[7] A. W. Bruno, D. Gallipoli, C. Perlot, and J. Mendes, "Mechanical behaviour of hypercompacted earth for building construction," *Mater. Struct.*, vol. 50, no. 2, p. 160, 2017.

[8] F. Champiré, A. Fabbri, J.-C. Morel, H. Wong, and F. McGregor, "Impact of relative humidity on the mechanical behavior of compacted earth as a building material," *Constr. Build. Mater.*, vol. 110, pp. 70–78, 2016.

[9] E. Araldi, E. Vincens, A. Fabbri, and J.-P. Plassiard, "Identification of the mechanical behaviour of rammed earth including water content influence," *Mater. Struct.*, vol. 51, no. 4, p. 88, 2018.

[10] Y.-J. Cui and P. Delage, "L'eau dans les sols non saturés," *Tech. l'ingérieur - Constr.*, vol. 1, no. C301, pp. 0–20, 2000.

[11] W. Gardner, "Some steady state solutions of the unsaturated moisture flow equation with application to evaporation from a water table," *Soil Sci.*, vol. 85, pp. 228–232, 1958.

[12] A. Corey, "The interrelation between gas and oil relative permeabilities," *Prod. Mon. 19*, vol. 19, pp. 38–41, 1954.

[13] W. Zillig, H. Janssen, J. Carmeliet, and D. Derome, "Liquid water transport in wood : Towards a mesoscopic approach," in *Research in Building Physics Engineering*, 2006, pp. 107–114.

[14] M. Cassan, *Les essais de perméabilité sur site dans la reconnaissance des sols*. 2005.

[15] J. Carmeliet, F. Descamps, and G. Houvenaghel, "A mutliscale network model for simulating moisture transfer properties of porous media," *Transp. Porous Media*, vol. 35, pp. 67–88, 1999.

[16] H. M. Kunzel, "Simultaneous heat and moisture transport in building components one - and two-dimensional calculation using simple parameters," Fraunhofer Institute of Building Physics, 1995.

[17] S. Roels *et al.*, "Interlaboratory Comparison of Hygric Properties of Porous Building Materials," *J. Therm. Envel. Build. Sci.*, vol. 27, no. 4, pp. 307–325, 2004.

[18] C. Feng, H. Janssen, Y. Feng, and Q. Meng, "Hygric properties of porous building materials : Analysis of measurement repeatability and reproducibility," *Build. Environ.*, vol. 85, pp. 160–172, 2015.

[19] S. Roels, J. Carmeliet, and H. Hens, "HAMSTAD, WP1: Final report Moisture Transfer Properties and Materials Characterization," Leuven, 2003.

[20] BSI, "BS-3921:1985 - Specification for clay bricks." p. 30, 1985.

[21] M. A. Wilson, M. A. Carter, and W. D. Hoff, "British Standard and RILEM water absorption tests: A critical evaluation," *Mater. Struct.*, vol. 32, pp. 571–578, 1999.

[22] M. Hall and Y. Djerbib, "Moisture ingress in rammed earth: Part 1—the effect of soil particle-size distribution on the rate of capillary suction," *Constr. Build. Mater.*, vol. 18, no. 4, pp. 269–280, May 2004.

[23] M. Raimondo, M. Dondi, D. Gardini, G. Guarini, and F. Mazzanti, "Predicting the initial rate of water absorption in clay bricks," *Constr. Build. Mater.*, vol. 23, no. 7, pp. 2623–2630, Jul. 2009.

[24] L. Soudani, A. Fabbri, J.-C. Morel, M. Woloszyn, P.-A. Chabriac, and A.-C. Grillet, “Assessment of the validity of some common assumptions in hygrothermal modeling of earth based materials,” *Energy Build.*, no. 116, pp. 498–511, 2016.

[25] P.-A. Chabriac, “Mesure du comportement hygrothermique du pisé,” ENTPE, Université de Lyon, France, 2014.

[26] M. Krus and A. Holm, “Simple method to approximate the liquid Transport coefficient describing the absorption and drying,” in *5th symposium ’Building Physics in the Nordic Countries - Göteborg, August 24-261*, 1999, pp. 241–248.

[27] I. Gomes, T. D. Gonçalves, and P. Faria, “Hygric Behavior of Earth Materials and the Effects of their Stabilization with Cement or Lime: Study on Repair Mortars for Historical Rammed Earth Structures,” *J. Mater. Civ. Eng.*, vol. 28, no. 7, p. p04016041, 2016.

[28] K. V. Bicalho, A. G. Correia, S. Ferreira, J. Fleureau, and A. M. Marinho, “Filter paper method of soil suction measurement,” in *XIII Panamerican Conference on Soil Mechanics and Geotechnical Engineering*, 2007.

[29] R. H. Brooks and A. T. Corey, “Hydraulic properties of porous media and their relation to drainage design,” *Trans. ASAE*, vol. 7, pp. 26–28, 1964.

[30] C. Miller, N. Yesiller, K. Yaldo, and S. Merayyan, “Impact of Soil Type and Compaction Conditions on Soil Water Characteristic,” *J. Geotech. Geoenvironmental Eng.*, 2002.

[31] V. Baroghel-Bouny, M. Thiery, F. Barberon, and G. Villain, “Assessment of transport properties of cementitious materials: a major challenge as regards durability?,” *Eur. J. Environ. Civ. Eng.*, vol. 11, no. 6, pp. 671–696, 2007.

[32] AFNOR, “NF EN ISO 12572.pdf.”

[33] R. Gummerson, C. Hall, and W. Hoff, “Water Movement in Porous Building Materia . ls--II . Hydraulic Suction and Sorptlvlty of Brick and Other Masonry Materials,” vol. 15, no. 3, pp. 101–108, 1980.

[34] S. Ghabezloo, J. Sulem, and J. Saint-Marc, “Evaluation of a permeability-porosity relationship in a low-permeability creeping material using a single transient test,” *Int. J. Rock Mech. Min. Sci.*, vol. 46, pp. 761–768, 2009.

[35] D. Breysse and B. Gérard, “Modelling of permeability in cement-based materials: Part 1 - Uncracked medium,” *Cem. Concr. Res.*, vol. 27, no. 5, pp. 761–775, 1997.

[36] N. Karagiannis, M. Karoglou, A. Bakolas, and A. Moropoulou, “Building Materials Capillary Rise Coefficient: Concepts, Determination and Parameters Involved,” *Build. Pathol. Rehabil.*, vol. 6, pp. 27–44, 2016.

[37] B. T. Lai, A. Fabbri, H. Wong, and D. Branque, “Poroelastic behaviour of fine compacted soils in the unsaturated to saturated transition zone,” *Comput. Geotech.*, vol. 69, pp. 627–640, 2015.

[38] A. Y. Pasha, A. Khoshghalb, and N. Khalili, “Pitfalls in Interpretation of Gravimetric Water Content–Based Soil-Water Characteristic Curve for Deformable Porous Media,” *Int. J. Geomech.*, vol. 16, no. 6, 2016.

[39] P.-A. Chabriac, A. Fabbri, J.-C. Morel, J.-P. Laurent, and J. Blanc-Gonnet, “A Procedure to Measure the in-Situ Hygrothermal Behavior of Earth Walls,” *Materials (Basel).*, vol. 7, pp. 3002–3020, 2014.

[40] M. T. Van Genuchten, “A Closed Form Equation for Predicting the Hydraulic Conductivity of Unsaturated Soils,” *Soil Sci. Soc. Am. J.*, vol. 44, no. 5, pp. 892–898, 1980.